

COMPRESSIBLE TURBULENCE

Sutanu Sarkar

Mechanical and Aerospace Engineering,
University of California at San Diego
9500 Gilman Drive, La Jolla, CA 92093
sarkar@ucsd.edu

ABSTRACT

Density (temperature) variation and a dilatational velocity component are hallmarks of compressible turbulence. After an introduction to turbulent flow examples where compressibility is important, attention is restricted to high-speed flows. The turbulent Mach number, M_t , can be significantly smaller than unity even in supersonic flows. Different approaches of low- M_t asymptotic analysis of the velocity and thermodynamic fluctuations are discussed. Compressibility effects are discussed through a review of four specific flows: isotropic turbulence, uniform shear flow, mixing layer and supersonic channel flow. The first three do not have a mean gradient in density or temperature. The magnitude of the dilatational component in direct simulations of isotropic turbulence is dependent on both initial conditions and turbulent Mach number, M_t . An acoustic mode with equipartition between kinetic and potential energies is observed. Turbulence in uniform shear flow and the mixing layer is inhibited with increasing Mach number. The pressure fluctuations play a particularly important role in this stabilizing effect and the gradient Mach number, M_g , is the relevant parameter that determines this effect. Supersonic channel flow has large gradients in mean properties that affect the log law in mean velocity as well as inner and outer scalings of the turbulent stresses. Some of the effects can be captured by appropriate weighting with local values of mean density and viscosity. However, there is an additional effect of pressure fluctuations on the Reynolds stresses which cannot be represented by such weighting.

INTRODUCTION

Compressible turbulence is concerned with turbulent flows where the assumption of a solenoidal velocity field or constant density/temperature cannot be made. Typical examples are high-subsonic-to supersonic flows where the mean Mach number is large, flows with large heat release such as combustion, and high-enthalpy flows as in hypersonics or laser applications. Significant changes in the thermodynamic and state variables are to be expected in such flows. The area of compressible turbulence is the study of how these changes couple with the velocity fluctuations. As with turbulence in the incompressible world, the study of compressible turbulence has included phenomenology, predictive modeling, simulations and first-principles theory ordered in descending number of contributions. An entry into the literature on compressible turbulence is provided by two monographs (Chassaing, Antonia, Anselmet, Joly, and Sarkar 2002; Smits and Dussauge 2006) and review papers (Bradshaw 1977; Lele 1994).

There have been many studies of compressible turbulence motivated by supersonic and hypersonic flight applications. The supersonic boundary layer has probably received the most attention in the compressible turbulence literature. At

high Mach number, there are large gradients in the temperature owing to viscous heating and the effect of concomitant density changes on the log-law, scaling laws for turbulence statistics and flow structures have been studied. The occurrence of shocks in external flows and propulsion systems of supersonic vehicles has prompted the study of the unsteady interaction of shocks with the turbulent boundary layer. Supersonic free shear layers and jets have received considerable attention motivated by the necessity of efficient fuel/air mixing within a short residence time in a scramjet (supersonic combustion ram jet) engine. Turbulence in supersonic jets has also been studied in the context of jet aeroacoustics.

In high-energy devices and explosions, there is rapid acceleration of density interfaces which leads to compressibility effects. Gravitational acceleration has strong stabilizing/destabilizing effects in environmental turbulent flows, but turbulence in such flows is excluded from the scope of compressible turbulence since the density change is small compared to the reference density. The situation with acceleration much larger than g introduces compressibility effects. Here, both the constant acceleration case corresponding to the Rayleigh Taylor problem and the impulsive case corresponding to the Richtmyer-Meshkov problem, have been studied. Density (temperature) changes are large in turbulent combustion even in the low-speed regime and originate instabilities of the flame such as the Darrieus-Landau instability and that due to differential diffusion of temperature and species. The effect of these instabilities on flame propagation in a premixed system is important to the efficiency and control of combustion. Mixing of fuel and oxidant in the presence of heat release is of interest in non-premixed combustion.

ANALYTICAL PRELIMINARIES

Understanding the influence of density variation in turbulent flow begins with the examination of the conservation equations for a compressible fluid. Mass conservation is governed by

$$\frac{\partial \rho}{\partial t} + (\mathbf{v} \cdot \nabla) \rho = -\rho \nabla \cdot \mathbf{v}. \quad (1)$$

Eq. (1) states that, not only is the density advected by the velocity field as any other scalar but it also increases (decreases) owing to volume compression (expansion). The dilatation, $d = \nabla \cdot \mathbf{v}$, is a kinematic quantity that is a new feature of compressible turbulence. Indeed, incompressible flow is defined by $d \equiv 0$. The magnitude of d relative to the vorticity magnitude ω , sometimes used as an analytical measure of compressibility, can be large in shocks and explosions.

The momentum equation is

$$\rho \frac{\partial \mathbf{v}}{\partial t} + \rho (\mathbf{v} \cdot \nabla) \mathbf{v} = -\nabla p + \nabla \cdot \boldsymbol{\tau} \quad (2)$$

where $\boldsymbol{\tau}$ is the viscous stress tensor. The density affects the velocity field through its presence in the inertia term on the l.h.s of Eq. (2). Consider inviscid flow where there is a balance between the first three terms. If the pressure gradient was the same as in the corresponding constant-density case, then high-density fluid would have lower magnitude of acceleration and the converse would be true for low-density fluid. On the other hand, if $\nabla p/\rho$ was identical to the corresponding constant-density value, then the velocity field would remain unmodified. Of course, neither of these two scenarios is correct but it motivates the derivation of an equation for p . Another motivation for closer study of p is that, in turbulent flow, it is the fluctuating pressure gradients which drive velocity fluctuations in directions other than the primary (mean flow) direction.

When density is changed owing to local heating, there are large changes in viscosity, $\mu(T)$, as in the supersonic boundary layer and in combustion. Thus, the local Reynolds number decreases approximately as $T^{-1.7}$, assuming constant mean pressure. In free shear flows, the change in Reynolds number is not expected to be a significant issue in high-Reynolds number flows but, since laboratory experiments and simulations are seldom at that limit, there may be some residual low- Re effects. In supersonic boundary layers, the decrease in Re has important consequences since the friction coefficient depends on Re . Furthermore, the region where the local Reynolds number, $\rho(y)U(y)y/\mu(y)$, is small enough for direct viscous effects on the turbulence to be important expands in size. Here, y is the wall-normal distance.

The equation for internal energy (equivalently temperature) for an ideal gas is

$$\rho \frac{\partial C_V T}{\partial t} + \rho(\mathbf{v} \cdot \nabla)T = -p \nabla \cdot \mathbf{v} + \Phi + \nabla \cdot (\kappa \nabla T) + \dot{Q}. \quad (3)$$

The temperature is advected by the velocity field and diffuses by heat conduction as in incompressible, non-isothermal flow. The pressure dilatation, $p \nabla \cdot \mathbf{v}$, and the viscous dissipation, Φ , are additional terms that account for exchange between mechanical and internal energy, and are no longer negligible when the turbulence is compressible. The pressure dilatation is the reversible part of the energy exchange and can be important in shocks while the viscous dissipation is the irreversible transfer to internal energy. \dot{Q} is the energy release associated with combustion.

The equation of state for a single-component ideal gas is

$$p = \frac{\rho R_g T}{W}. \quad (4)$$

where W is the molecular weight. It follows from Eq. (4) that

$$\frac{dp}{p} = \frac{d\rho}{\rho} + \frac{dT}{T}. \quad (5)$$

The origin of thermodynamic fluctuations determines the relative magnitude of the terms in the above equation. For example, in the entropy mode $dp/p \ll d\rho/\rho, dT/T$. Consequently density and temperature fluctuations have a correlation coefficient approaching unity. The acoustic mode has isentropic fluctuations so that all terms in Eq. (5) are of comparable magnitude.

The vorticity, $\boldsymbol{\omega}$, occupies a paramount position in the study of turbulence mainly because the vortex stretching term underlies our physical picture of a cascade from large to small scales in turbulence. Vortical motion is effective in accomplishing large-scale stirring and transport, and the notion of eddies in turbulence is almost synonymous with

vortices. At the same time it is worth noting that the strain rate tensor, the other component of the velocity deformation tensor, is also important because mixing at the molecular level is efficiently accomplished by the amplification of scalar gradients in a compressive strain field. The equation for $\boldsymbol{\omega}$ reads as

$$\begin{aligned} \frac{D\boldsymbol{\omega}}{dt} &= (\boldsymbol{\omega} \cdot \nabla)\mathbf{v} + \nabla \times \frac{\nabla \cdot \boldsymbol{\tau}}{\rho} - \boldsymbol{\omega} \nabla \cdot \mathbf{v} + \frac{\nabla \rho \times \nabla p}{\rho^2} \\ &\approx (\boldsymbol{\omega} \cdot \nabla)\mathbf{v} + \nu \nabla^2 \boldsymbol{\omega} - \boldsymbol{\omega} \nabla \cdot \mathbf{v} + \frac{\nabla \rho \times \nabla p}{\rho^2}. \end{aligned} \quad (6)$$

The second line of the above equation is a simplification that follows by neglecting variation of fluid properties in the viscous stress tensor. The last two terms in Eq. (6) constitute the explicit effects of compressibility. The third term on the r.h.s represents the increase (decrease) of vorticity by compression (expansion) while the fourth term represents the so-called baroclinic torque. In an inviscid and barotropic process where p is solely a function of ρ , the quantity $\boldsymbol{\omega}/\rho$ is conserved showing that the vorticity field is strongly linked to the density.

There are different choices for writing the equation for pressure. The equation for temperature, Eq. (3), can be converted to the following equation for the thermodynamic pressure using the equation of state:

$$\frac{\partial p}{\partial t} + (\mathbf{v} \cdot \nabla)p = -\gamma p \nabla \cdot \mathbf{v} + (\gamma-1)\Phi + (\gamma-1)\nabla \cdot (\kappa \nabla T) + (\gamma-1)\dot{Q}. \quad (7)$$

Another possibility is to take the divergence of the momentum equation and obtain an equation for the pressure,

$$\nabla^2 p = -\frac{\partial^2(\rho u_i u_j)}{\partial x_i \partial x_j} + \frac{\partial^2 \tau_{ij}}{\partial x_i \partial x_j} + \frac{\partial^2 \rho}{\partial t^2}. \quad (8)$$

An equation for the fluctuating pressure can be derived (Chassaing *et al.* 2002) from Eq. (8). In the constant-density case, it simplifies to a Poisson equation for the pressure. In the case of a compressible fluid, the following relationship between changes in density, pressure and entropy,

$$d\rho = \frac{1}{c^2} dp - \frac{\rho}{C_p} dS,$$

is used to convert the $\partial^2 \rho / \partial t^2$ term in Eq. (8) to a term involving $\partial^2 p / \partial t^2$ so that a *wave equation* for pressure results. The change from infinite speed of propagation to finite speed of pressure waves has important physical consequences. If τ is the decorrelation time for velocity fluctuations of an eddy of size l , the pressure fluctuation generated inside the eddy can travel only a finite distance, $c\tau$, instead of the instantaneous communication throughout the flow domain allowed by the incompressible assumption. Furthermore, the zone of influence, instead of being spherical, is anisotropic in shear flow as discussed by Papamoschou(1993), see Fig. 1.

Decomposition of the governing equations

Kovaszny (1953) was probably the first to attempt a systematic decomposition of the Navier-Stokes equation to identify deviations from incompressibility. He identified the following three modes:

$$\begin{aligned} \text{vorticity mode :} & \quad \boldsymbol{\omega}' \neq 0 & \quad \rho' = p' = s' = 0 \\ \text{acoustic mode :} & \quad \boldsymbol{\omega}' = s' = 0 & \quad \rho' = p' \neq 0 \\ \text{entropy mode :} & \quad \boldsymbol{\omega}' = p' = 0 & \quad s' = \rho' \neq 0 \end{aligned} \quad (9)$$

By *linearizing* the Navier-Stokes equations with respect to a stationary state, he showed that these three modes do

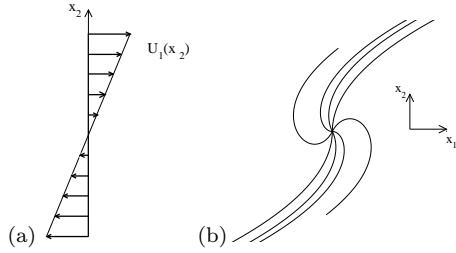


Figure 1: Sketch of pressure wave propagation in uniform shear flow: (a) Mean velocity profile, (b) Ray trajectories emanating from source at initial angular spacings of $\pi/4$. From Thacker *et al.*(2007).

not interact in that approximation and each satisfies its own equation. One lasting contribution of the Kovaszny modal decomposition is that it clearly identifies the qualitative difference in density fluctuations depending on its origin i.e., ρ' in the acoustic mode satisfied a wave equation while ρ' in the entropy mode satisfies a diffusion equation. But, the modal decomposition has limitations since, first, vortical turbulence itself is a nonlinear phenomenon and, second, compressible turbulence is the problem where the interaction terms between the various modes are important.

Lighthill (1952) proposed the acoustic analogy by a physically-based interpretation of the wave equation for pressure. He assumed that the r.h.s term involving the velocity field occupied a compact domain, was governed by incompressible turbulence phenomenology, and constituted an equivalent compact acoustic source. The density (pressure) fluctuations i.e; the acoustics external to the compact domain was taken to be the *effect* of this source. By construction, Lighthill considered the one-way coupling from turbulence to density fluctuations, thereby bypassing the problem of how compressibility influences turbulence.

There have been proposals to decompose the compressible Navier-Stokes equations into interacting “compressible” and “incompressible” components through a theory valid for small M_t , the Mach number based on *fluctuations*. The interest in low M_t theory arises because M_t is small even in supersonic flows. The Lighthill acoustic analogy can be viewed as one such effort which, although a one-way interaction, serves its purpose, namely, prediction of noise generated by subsonic flow. A generic decomposition proceeds as follows. The velocity, density and pressure are decomposed by

$$\begin{aligned} \mathbf{v} &= \mathbf{v}^{\mathbf{I}}(\mathbf{x}, t) + \mathbf{v}^{\mathbf{C}}(\mathbf{x}, t), \\ \rho_{total} &= \rho_0 + \rho, \\ p_{total} &= P_0 + p(\mathbf{x}, t) = P_0 + p^{\mathbf{C}}(\mathbf{x}, t) + p^{\mathbf{I}}(\mathbf{x}, t). \end{aligned} \quad (10)$$

Here ρ_0 and P_0 are the reference thermodynamic density and pressure. A kinematic decomposition for the velocity is the Helmholtz decomposition that is convenient when the turbulence is homogeneous: $\mathbf{v}^{\mathbf{I}}$ is solenoidal and rotational and $\mathbf{v}^{\mathbf{C}}$ is irrotational and dilatational.

Decomposition of the pressure is not as clear cut as that for the velocity. There appears to be two main possibilities as will be discussed below: the *acoustic decomposition* that allows pressure waves traveling with the speed of sound at lowest order and the *non-acoustic* decomposition that does not. Mathematically, the first approach retains the acoustic time scale, $\tau_A = l/c$, in the limit $M_t \rightarrow 0$ of the equation governing $\mathbf{v}^{\mathbf{C}}$, while the second does not. The acoustic time scale is related to the convective time scale, $\tau = l/u$, by

$\tau_A = \tau M_t$ and is a fast time scale. Here, u and l characterize the velocity and length scales of the fluctuations.

Acoustic decomposition.

A decomposition (Erlebacher, Hussaini, Kreiss, and Sarkar 1990) that retains the acoustic mode as $M_t \rightarrow 0$ is as follows. These authors neglect heat conduction and viscous terms, assume an isentropic relation between thermodynamic fluctuations, and retain terms up to first order in the pressure fluctuation, p , to obtain:

$$\begin{aligned} \frac{\partial \mathbf{v}}{\partial t} + (\mathbf{v} \cdot \nabla) \mathbf{v} + \frac{1}{\rho_0} \nabla p &= 0 \\ \frac{\partial p}{\partial t} + (\mathbf{v} \cdot \nabla) p + \gamma(P_0 + p) \nabla \cdot \mathbf{v} &= 0 \end{aligned} \quad (11)$$

They define $\mathbf{v}^{\mathbf{I}}$ and $p^{\mathbf{I}}$ as the solution of the incompressible flow problem,

$$\begin{aligned} \nabla \cdot \mathbf{v}^{\mathbf{I}} &= 0 \\ \frac{\partial \mathbf{v}^{\mathbf{I}}}{\partial t} + (\mathbf{v}^{\mathbf{I}} \cdot \nabla) \mathbf{v}^{\mathbf{I}} &= -\frac{1}{\rho_0} \nabla p \\ \nabla^2 p^{\mathbf{I}} &= -\frac{\partial^2 v^{\mathbf{I}}_i v^{\mathbf{I}}_j}{\partial x_i \partial x_j} \end{aligned} \quad (12)$$

An evolution equation for $(\mathbf{v}^{\mathbf{C}}, p^{\mathbf{C}})$ is obtained by inserting the decomposition, Eq. (10), into Eq. (11) and then subtracting Eq. (12) from the result. The following equations for the compressible mode ensue:

$$\begin{aligned} \frac{\partial \mathbf{v}^{\mathbf{C}}}{\partial t} + \frac{1}{\rho_0} \nabla p^{\mathbf{C}} + \dots &= 0 \\ \frac{\partial p^{\mathbf{C}}}{\partial t} + \gamma P_0 \nabla \cdot \mathbf{v}^{\mathbf{C}} + \dots &= -\frac{\partial p^{\mathbf{I}}}{\partial t} - \mathbf{v}^{\mathbf{I}} \cdot \nabla p^{\mathbf{I}} \end{aligned} \quad (13)$$

where the \dots in Eq. (13) denote the interaction terms between the incompressible and compressible variables. On the fast time scale, the convective terms are neglected to give a homogeneous system, the so-called acoustic truncation:

$$\begin{aligned} \frac{\partial \mathbf{v}^{\mathbf{C}}}{\partial t} + \frac{1}{\rho_0} \nabla p^{\mathbf{C}} &= 0 \\ \frac{\partial p^{\mathbf{C}}}{\partial t} + \gamma P_0 \nabla \cdot \mathbf{v}^{\mathbf{C}} &= 0 \end{aligned} \quad (14)$$

The system, Eq. (14), is hyperbolic with strongly asymmetric coefficients. Erlebacher *et al.*(1990) have shown that the above decomposition describes the evolution of the dilatation and pressure in compressible isotropic turbulence. The compressible velocity, $\mathbf{v}^{\mathbf{C}}$, is known *if* $p^{\mathbf{C}}$ is known. Let P_0 be the ambient pressure. From Eq. (13), it is seen that $p^{\mathbf{I}}$ forces $p^{\mathbf{C}}$ leading to the possibility that $p^{\mathbf{C}}/P_0 = O(p^{\mathbf{I}}/P_0) = O(M_t^2)$; the consequences of such an assumption on the scaling laws for the dilatational variance and pressure-dilatation correlation have been explored (Sarkar, Erlebacher, Hussaini, and Kreiss 1991; Sarkar 1992).

Nonacoustic decomposition.

The second possibility is to ignore the fast acoustic time scale. Ristorcelli (1997) does so and further assumes $p^{\mathbf{C}}/p^{\mathbf{I}} = O(M_t^2)$ for consistency. He then obtains the lowest order equations to be the incompressible flow equations, Eq. (12), plus the linearized isentropic relationship, $dp^{\mathbf{I}}/p_0 = \gamma d\rho/\rho_0$, between the incompressible flow pressure and the density fluctuation. The dilatation appears in the

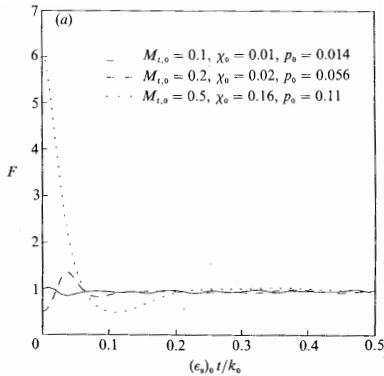


Figure 2: Evolution of F in isotropic turbulence. From Sarkar *et al.* (1991).

mass conservation equation at next order,

$$\begin{aligned} d = \nabla \cdot \mathbf{v} &= -\frac{1}{\rho_0} \frac{D\rho}{Dt} \\ &= -\frac{1}{\gamma p_0} \frac{Dp^I}{Dt} \end{aligned} \quad (15)$$

Density (temperature) fluctuations directly related by the isentropic relationship to the incompressible flow pressure, as in Eq. (15), are conventionally called pseudo-sound to distinguish them from sound waves which, although also isentropic, propagate in space. The relationship, Eq. (15), between dilatation and pressure has been used to model the dilatational variance and pressure-dilatation correlation (Zeman 1991; Ristorcelli 1997).

Rehm and Baum (1978) considered low-Mach number combustion and approximated the equations to avoid the fast acoustic time scale. The energy equation, Eq. (7), is rearranged:

$$d = \nabla \cdot \mathbf{v} = \frac{1}{\gamma p_0} \left(-\frac{dp^C}{dt} + (\gamma - 1)(\dot{Q} + \nabla \cdot (\kappa \nabla T) + \Phi) \right) \quad (16)$$

The term, dp^C/dt , is obtained by integrating the above equation over the volume with the appropriate boundary conditions. Then, Eq. (16) can be interpreted as an explicit equation for the dilatation d . In the case of non-reacting flows ($\dot{Q} = 0$) but with large temperature differences i.e. $dT/T \gg dp/p = O(M_t^2)$, the term dp^C/dt on the r.h.s can be neglected. Such a simplification was successfully used (Borodai and Moser 2001) to separate non-acoustic dilatation from acoustic dilatation in a DNS database of a supersonic boundary layer.

ISOTROPIC TURBULENCE

Isotropic turbulence in a box is an idealized initial value problem which is particularly useful to study the interaction of solenoidal and dilatational velocity components as well as deviations from incompressible behavior. Assume an ideal gas. For a given initial spectral shape, the parameters that measure compressibility are: M_t , the fraction of kinetic energy in the dilatational mode $\chi = q^{C^2}/q^2$, and the r.m.s thermodynamic fluctuations: $\rho'/\langle \rho \rangle$ and $T'/\langle T \rangle$. There have been several numerical simulations of isotropic turbulence spanning this wide parameter range since the first study (Passot and Poquet 1987) which employed 2-D equations.

Insofar as the energetics are concerned, the influence of compressibility on the decay rate of the turbulent kinetic energy, K , is of interest. The equation governing K in isotropic

turbulence is:

$$\frac{\partial K}{\partial t} = -\epsilon + \langle p'd' \rangle = -(\epsilon_I + \epsilon_d) + \langle p'd' \rangle, \quad (17)$$

where $\epsilon_s = (\langle \mu \rangle / \langle \rho \rangle) \langle \omega'_i \omega'_i \rangle$ is the solenoidal dissipation rate and $\epsilon_d = (4/3) \langle \mu \rangle / \langle \rho \rangle \langle d'd' \rangle$ is the dilatational dissipation rate. If ϵ_s remains unaffected by compressibility, then ϵ would be augmented owing to ϵ_d . Simulations of unforced isotropic turbulence generally find that there is a small-to-modest increase in ϵ which is dependent on M_t and the choice of initial conditions.

The role of the acoustic mode in the evolution from initial conditions has been investigated (Sarkar, Erlebacher, Hussaini, and Kreiss 1991). They solved the initial value problem of random fluctuations that evolve according to the acoustic truncation, Eq. (14), to find that the initial data evolves on the fast time scale, $\tau_A = l/c$ towards equipartition between kinetic and potential energy in the compressible component,

$$\begin{aligned} F &= \frac{\gamma M_t^2 \chi}{\langle p'^{C^2} \rangle / \langle p \rangle^2} \\ &= \frac{\langle \rho \rangle q^{C^2}}{\langle p'^{C^2} \rangle / (\gamma \langle p \rangle)} = \frac{\text{K.E.}}{\text{P.E.}} \rightarrow 1 \end{aligned} \quad (18)$$

The rapid evolution, on the acoustic time scale, of F towards unity in isotropic turbulence (see Fig. 2) was demonstrated for M_t up to 0.5 (Sarkar *et al.* 1991). Later in time, F was found to oscillate around unity while the variance of pressure and dilatation decayed at the slow eddy-turnover time scale. The relation $F \rightarrow 1$ was also observed (Cai, O'Brien, and Ladiende 1997) for the situation when the entropy mode dominated initially i.e. initial temperature (density) fluctuations were anti-correlated and were also much larger than pressure fluctuations. It appears that Eq. (18) is a good approximation for the acoustic mode. Nevertheless, to estimate q_c (equivalently d), one must make a statement about p^C . If we take $p^C / \langle p \rangle = O(p^I / \langle p \rangle) = (M_t^2)$ because p^C is forced by p^I , it follows that $\chi \propto M_t^2$. The implications of such a scaling is that $\epsilon_d \propto \epsilon_s M_t^2$. However, if we postulate that $p^C / p^I \rightarrow 0$ as $M_t \rightarrow 0$, for example, by taking $p^C / \langle p \rangle = O(M_t^3)$ then $\chi = O(M_t^4)$. The initial data can be chosen to minimize acoustic effects and the dilatational variance and therefore, ϵ_d , depends on the initial conditions (Ristorcelli and Blaisdell 1997). For instance, one could choose a solenoidal velocity field, zero density fluctuations, and a pressure field that satisfies a Poisson equation. In this case too, the dilatation builds up on an acoustic time scale but its magnitude is reduced relative to a case where $p^C(t=0)$ is comparable to $p^I(t=0)$.

There is the intriguing possibility of eddy shocklets, localized jumps in the fluctuating field typical of a shock wave. A model for the dilatational dissipation based on eddy shocklets has been proposed by Zeman (1990). Eddy shocklets are found in isotropic turbulence if M_t and Re are sufficiently large, especially in 2-D simulations. However, they are sparse and infrequent in 3-D simulations up to $M_t = 0.5$, and the dilatational dissipation associated with them is small compared to the solenoidal dissipation rate (Lee, Lele, and Moin 1991).

The eddy damped quasi-normal Markovian (EDQNM) model, has been used to simulate forced isotropic compressible turbulence at high Reynolds number (Bertoglio, Bataille, and Marion 2001). Approximate equipartition between dilatational energy and pressure was observed at each wave number i.e. $F(k) \simeq 1$, and the dilatational dissipation

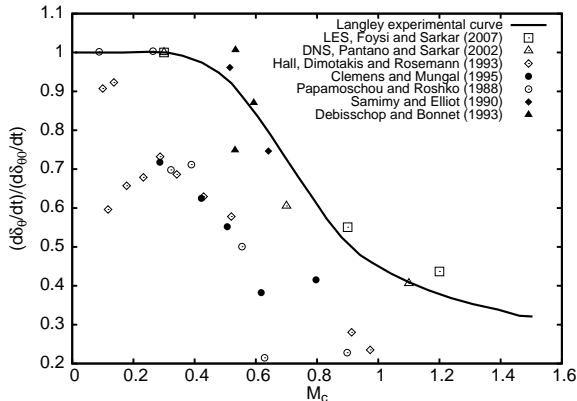


Figure 3: Growth rate of the mixing layer as a function of M_c .

was found to be proportional to M_t^2 . The solenoidal velocity spectrum followed a $k^{-5/3}$ law while both, dilatational and pressure spectra, showed a steep $k^{-11/3}$ law.

HIGH-SPEED MIXING LAYER

The decrease in thickness growth rate of the mixing layer as a function of convective Mach number, $M_c = (U_1 - U_2)/(c_1 + c_2)$, has been observed in laboratory experiments (Papamoschou and Roshko 1988; Elliot and Samimy 1990; Hall, Dimotakis, and Rosemann 1993; Debisschop and Bonnet 1993; Clemens and Mungal 1995) and DNS (Vreman, Sandham, and Luo 1996; Freund, Lele, and Moin 2000; Pantano and Sarkar 2002). It is remarkable that, in the absence of mean density variation, the decrease in thickness growth rate is so strong, about a factor of 3 reduction at $M_c = 1$. Fig. 3 is a compilation of experimental and numerical data. The Langley curve, a consensus of various laboratory data, is regarded as representative of the influence of M_c when the two streams have the same composition; data on Fig. 3 with significantly lower growth rate correspond to gases with substantially different density.

DNS of the temporally evolving mixing layer has been used to explore the reasons for the stabilizing effect of M_c on the mixing layer growth rate as summarized below. Vreman *et al.* (1996) performed DNS for $M_c = 0.2, 0.6, 0.8, 1.2$. Under the assumption of zero normal velocity and negligible molecular dissipation of the mean flow, they showed that the turbulent production, integrated over the mixing layer, is proportional to the growth rate of the momentum thickness. Thus, the reduced growth rate is equivalent to a reduced production i.e. reduced $R_{12}/\Delta u^2$. The r.m.s pressure fluctuation, $p_{rms}/\langle \rho \rangle \Delta u^2$, was found to be reduced and so was the pressure-strain correlation, Π_{11} . Vreman *et al.* (1996) also proposed a coherent vortex model with the azimuthal velocity constrained to be less than or equal to the sonic value to explain the reduced pressure.

Freund *et al.* (2000) performed DNS of an annular mixing layer over the range $0.1 \leq M_c \leq 1.8$. They also found that the pressure fluctuations and the pressure-strain term were reduced as a function of M_c . The transverse length scale, l_2 , determined by the two-point correlation of the radial velocity fluctuation, was taken to be a large-eddy length scale and it was found that l_2 decreased with increasing M_c . The gradient Mach number, $M_g = Sl_2/c$ increased linearly with M_c up to $M_g = 0.75$ and then, after exhibiting a sublinear growth, saturated at $M_g \simeq 2$.

Pantano and Sarkar (2002) performed DNS of the plane

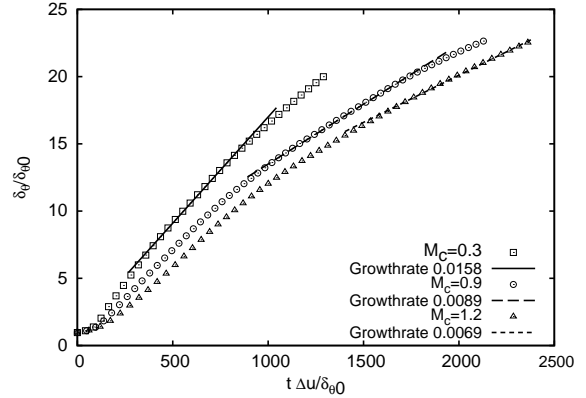


Figure 4: Evolution of the momentum thickness.

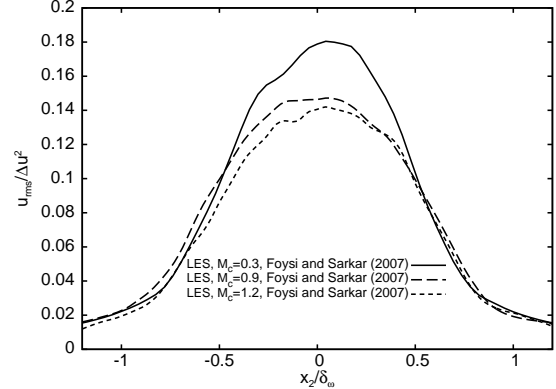


Figure 5: Profiles of streamwise turbulence intensity.

mixing layer for $M_c = 0.3, 0.7, 1.1$. They reconfirmed the decrease in pressure fluctuations and pressure-strain correlation with increased M_c and performed an analysis of the wave equation for p' that predicted a decrease. This analysis was performed at the centerline of the mixing layer (where $\langle u \rangle = 0$) after assuming local homogeneity of the turbulence, neglecting mean convection in the wave operator and, based on the DNS data, assuming an exponential decorrelation in time of two-time turbulence correlations. These authors obtained the following expression for the pressure-strain correlation:

$$\frac{\Pi_{ij}}{\Pi_{ij}^I} = 1 - \frac{1}{\Pi_{ij}^I} \int_{-\infty}^{\infty} \frac{\Psi_{ij}^I(\mathbf{k})}{1 + (c_o \tau_I k)^2} d\mathbf{k}. \quad (19)$$

Here, Π_{ij}^I is the pressure-strain correlation in the incompressible case and $\Psi_{ij}^I(\mathbf{k})$ is its Fourier transform. Eq. (19) shows that all components of the pressure-strain tensor show *monotone decrease* with decreasing speed of sound in compressible shear flow. Since the turbulence time scale of a wave number k is related to its turnover time i.e. $\tau_I k \simeq 1/u(k)$, Eq. (19) implies that energy-containing modes with higher $M(k)^2 = u(k)^2/c^2$ have higher relative reduction. DNS has also been employed to investigate the effect of density ratio, $s = \rho_2/\rho_1 = 1, 2, 4, 8$, at $M_c = 0.7$ (Pantano and Sarkar 2002). They found that, at $s = 8$, the momentum thickness growth rate decreased to 40% of the value at $s = 1$. The reason was identified to be the shift of the dividing stream line to the low-density side that decreases $\langle \rho \rangle > R_{12}$ rather than a decrease in R_{12} .

LES of the high-speed mixing layer

The capabilities of LES to capture the observed dependence on M_c have been explored in a recent study by Foyi and Sarkar (2007). The subgrid stress tensor, $\tau_{ij} = \widetilde{u_i u_j} - \widetilde{u_i} \widetilde{u_j}$, was modeled using the dynamic Smagorinsky

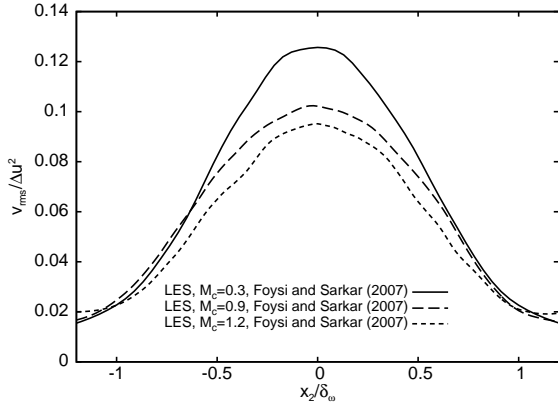


Figure 6: Profiles of cross-stream turbulence intensity.

M_c	$Re_{\omega,0}$	N_x	N_y	N_z	$\frac{L_x}{\delta_{\theta 0}}$	$\frac{L_y}{\delta_{\theta 0}}$	$\frac{L_z}{\delta_{\theta 0}}$
0.3	705	768	48	193	1720.4	108	344
0.9	705	768	96	193	1720.4	108	344
1.2	705	768	96	193	1720.4	108	344

Table 1: Parameters, Foyasi and Sarkar (2007).

model. The filtered internal energy equation was solved with the subgrid term given by the sum of the subgrid dissipation and a eddy diffusivity model for the subgrid heat flux:

$$-\tau_{ij} \frac{\partial \tilde{u}_i}{\partial x_j} + \frac{\bar{\rho} \nu_t}{Pr_t} \frac{\partial \tilde{T}}{\partial x_j}. \quad (20)$$

The parameters of LES cases are shown in Table 1. The LES grid of approximately 14 million grid points is comparable to the 17 million points DNS grid (Pantano and Sarkar 2002), but the box size is 5 times larger in the streamwise direction and 4 times larger in the cross-stream direction to allow a larger time interval of self-similar evolution. The final Reynolds number based on the vorticity thickness is $Re_{\omega,f} \simeq 16,000$. The LES results in Figure 4 show regions of self-similar growth in each case with the slope decreasing with increasing M_c . The thickness growth rates of the LES cases (open squares in Fig. 3) are close to but slightly higher than the Langley curve. Figs. 5-6 show profiles of streamwise, cross-stream and spanwise turbulence intensity. The Mach number does not affect the shape of the profiles or the usual ordering of the turbulence intensities of streamwise > spanwise > cross-stream. However the peak values of all the turbulence intensities decrease with increasing M_c . In the incompressible self-similarly evolving mixing layer, the centerline pressure fluctuations, $p_{rms}/(\rho_0 \Delta u^2)$, and the pressure-strain correlation integrated across the mixing layer, $\bar{\Pi}_{ij}/(\rho_0 \Delta u^3)$, become invariant with time. These quantities, normalized by their values at $M_c = 0.3$, are shown in Fig. 7. In both the DNS and LES, the r.m.s. pressure and all components of the pressure-strain correlation show monotone decrease.

The anisotropy, b_{ij} , of the Reynolds stress tensor is a measure of the partition of the turbulent energy into the three coordinate directions. The effect of compressibility on b_{ij} was ambiguous in earlier studies. The earlier DNS studies by Vreman *et al.* (1996) and Freund *et al.* (2000) show that the normal stress anisotropy increases with increasing M_c because R_{11} decreases less than the other components. However, the more recent DNS (Pantano and Sarkar 2002) show that such a trend occurs during the transient but, later in time during the self-similar stage, the components of b_{ij} are relatively unaffected by M_c . The LES results agree with the DNS data as shown in Table 2.

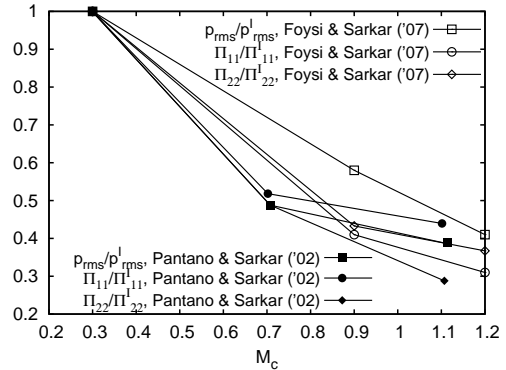


Figure 7: Influence of M_c on centerline r.m.s pressure fluctuations and pressure-strain rate correlation integrated over the mixing layer.

M_c	b_{11}	b_{22}	b_{12}	M_c	b_{11}	b_{22}	b_{12}
0.3	0.14	-0.06	0.18	0.3	0.13	-0.075	0.16
0.7	0.15	-0.10	0.15	0.9	0.14	-0.10	0.15
1.1	0.14	-0.10	0.16	1.2	0.15	-0.10	0.15

Table 2: The Reynolds stress anisotropy in the self-similar region: left table from DNS of Pantano and Sarkar (2002), right table from LES of Foyasi and Sarkar (2007).

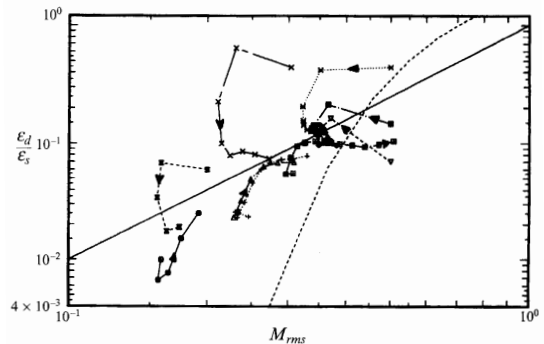


Figure 8: Scaling of the dilatational dissipation: symbols, various cases, — model of Sarkar *et al.* (1991), - - - model of Zeman (1993). From Blaisdell *et al.* (1993).

UNIFORM SHEAR FLOW

Uniform shear (also called homogeneous shear flow) has mean velocity $(Sx_2, 0, 0)$ with $S = \text{constant}$, and is a useful model problem because, although a shear flow, the turbulence is homogeneous. The first DNS (Feiereisen, Reynolds, and Ferziger 1981) was unable to draw conclusions about the influence of compressibility. Later, Blaisdell, Mansour and Reynolds (1991, 1993) and Sarkar, Erlebacher and Hussaini (1991) conducted independent DNS studies which identified significant changes with increasing Mach number. The growth rate of the turbulent kinetic energy,

$$\Lambda = \frac{1}{SK} \frac{dK}{dt}$$

was found to decrease systematically with increasing initial M_t in both studies, to approximately 65% of the incompressible value at $M_t \simeq 0.4$. Explicit dilatational terms, $\langle p'd' \rangle - \epsilon_d$, on the r.h.s of the K equation were found to be responsible for the reduced growth rate. Unlike isotropic turbulence, the results after an initial transient were fairly insensitive to the initial data because the mean shear, S , couples the dilatation and spanwise vorticity fluctuation in the linearized inviscid equations (Blaisdell, Mansour, and Reynolds 1993). Both studies found that the DNS data followed the model of Sarkar *et al.* (1991), $\epsilon_d \simeq 0.5\epsilon_s M_t^2$,

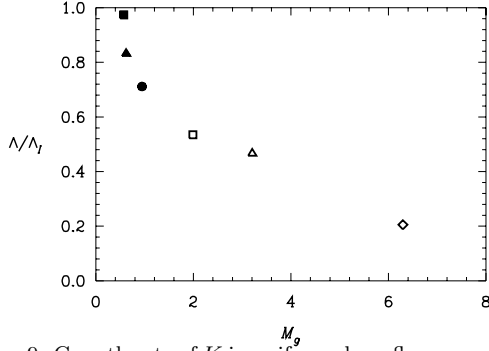


Figure 9: Growth rate of K in uniform shear flow normalized by its incompressible value. Open symbols correspond to series A and filled symbols to series B. From Sarkar (1995).

at low M_t , but there was a saturation at higher M_t to $\epsilon_d/\epsilon_s \simeq 10-15\%$. Fig. 8 illustrates the scaling of the dilatational dissipation. Eddy shocklets were found in the DNS of Blaisdell *et al.* (1993) and the intermediate values of dilatation that occurred at the peripheries of the shocklets were found to contribute significantly to ϵ_d .

Sarkar (1995) performed additional simulations to isolate the effect of the gradient Mach number, $M_g = Sl_2/c$, from that of M_t . In series A, the gradient Mach number was varied in the range $0.22 < M_{g0} < 1.32$ keeping $M_{t0} = 0.4$ constant while, in series B, $0.13 < M_{t0} < 0.40$ keeping $M_{g0} = 0.22$ constant. Fig. 9 shows that a large reduction in growth rate occurs in series A. The evolution equation for K in homogeneous shear flow can be rewritten as:

$$\begin{aligned} \Lambda &= \frac{P}{SK} - \frac{\epsilon_s}{SK} - \frac{(\epsilon_d - \langle p'd' \rangle / \langle \rho \rangle)}{SK} \\ &= \frac{P}{SK}(1 - X_\epsilon), \end{aligned} \quad (21)$$

where P is the turbulent production and, in the second line, X_ϵ lumps together all terms other than shear production. It was found that P/SK exhibits a large decrease from its incompressible value of 0.15 to 0.06 while $X_\epsilon \simeq 0.65 \pm 0.05$ changes little between cases. This result was independently verified using DNS (Simone, Coleman, and Cambon 1997). Thus, if P/SK is interpreted as the analog of normalized production in the inhomogeneous mixing layer, the stabilizing effect of compressibility is due to reduced production in both flows. The magnitude of shear stress anisotropy decreases and those of the normal stress anisotropies increase with increasing M_g in series A. Series B exhibits a moderate reduction of Λ similar to the earlier simulations. Furthermore, similar to these earlier studies, the reduction in series B, unlike that in series A, is found to be mainly due to $\langle p'd' \rangle$ and ϵ_d .

The evolution of pressure fluctuations in homogeneous shear flow was reported by Sarkar (1996). Fig. 10 shows that compressibility inhibits the pressure fluctuations, similar to the trend seen in DNS and LES of the mixing layer. In Case A4 with the largest M_g , the r.m.s. pressure exhibits a monotone decrease after $St = 3$. Interestingly, the cross-stream velocity fluctuations, $\langle v'^2 \rangle$, also exhibits a monotone decrease after $St = 4$. A connection between cross-stream perturbations and pressure perturbations has been identified in a linearized analysis (Friedrich and Bertolotti 1997). The reduction of pressure fluctuations was also noted and terms in the pressure-variance equation examined in the DNS by Hamba (1999).

Simone, Coleman and Cambon(1997) performed both DNS and an RDT analysis. The RDT analysis involved the

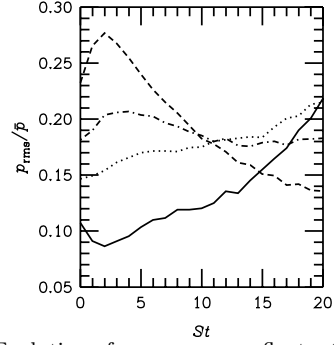


Figure 10: Evolution of r.m.s. pressure fluctuations in homogeneous shear flow : —, case A1;, case A2; - - -, case A3; - · -, case A4. From Sarkar (1996).

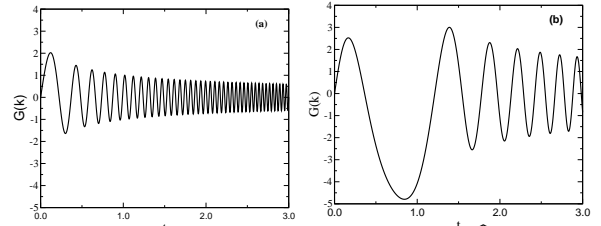


Figure 11: Time evolution of Green's functions \hat{G} in uniform shear flow at $M_t = 0.2$ and $M_g = 1.0$. Two values of the angle of propagation ϕ in the shear ($x_1 - x_2$) plane and with respect to the downstream x_1 direction are shown: (a) $\phi = 15$ degrees, (b) $\phi = 105$ degrees.

linearized, inviscid equations for velocity, \mathbf{v} , and pressure, p , which were transformed to wave number space and then numerically solved. An important finding was that both RDT and DNS showed that, for $St < 4$, the growth rate Λ increased with increasing M_g and, for $4 < St < 15$, there was a stabilizing effect i.e. Λ decreased with increasing M_g . Thus, linear RDT analysis is successful in qualitatively predicting the stabilizing effect of compressibility. There were some discrepancies between RDT and DNS too: RDT over-predicted the growth rates compared to DNS; the long-time values of b_{12} in the RDT solution appear to asymptote to a unique value while those in the DNS remain separated according to the initial value of M_g . Nonlinear and dissipative effects are evidently important for the long-time evolution.

Thacker, Sarkar and Gatski (2007) performed a Green's function based analysis of the pressure fluctuations. The following nondimensional equation governs pressure fluctuations in a flow with constant mean velocity gradients:

$$\begin{aligned} &\left[\left(M_t \frac{\partial}{\partial t} + M_g \tilde{U}_j \frac{\partial}{\partial x_j} \right)^2 - \frac{\partial^2}{\partial x_j \partial x_j} \right] p' \\ &= 2 \left(\frac{M_g}{M_t} \right) \frac{\partial \tilde{U}_i}{\partial x_j} \frac{\partial (\rho u_j'')}{\partial x_i} + \left(\frac{M_g}{M_t} \right)^2 \frac{\partial \tilde{U}_i}{\partial x_j} \frac{\partial \tilde{U}_j}{\partial x_i} \rho' \\ &\quad + \frac{\partial^2}{\partial x_i \partial x_j} \left[\langle \rho \rangle (u_i'' u_j'' - \widetilde{u_i'' u_j''}) + \rho' u_i'' u_j'' \right]. \end{aligned} \quad (22)$$

Here, $M_t = u_0/c_0$ and $M_g = Sl_0/c_0$ are the reference values for turbulent Mach number and gradient Mach number, respectively. It can be seen that both M_t and M_g appear independently in the wave operator on the l.h.s of the above equation and that, in the limit $M_t, M_g \rightarrow 0$, the Poisson equation with rapid and slow forcing terms that is familiar from incompressible flow is recovered.

Thacker *et al.*(2007) derived an exact expression for the Green's function for the convected wave operator on the l.h.s of Eq. (22) in wave number space. The Green's function,

Eqs. (27)-(28) of Thacker *et al.*(2007), is a combination of parabolic cylinder functions. In the absence of convection by mean flow on the l.h.s, the shear-free Green's function (Pantano and Sarkar 2002) is recovered which corresponds to undamped oscillation with the acoustic time period $2\pi/c_k$. Mean shear introduces a qualitative change: both the amplitude and frequency of the oscillation are variable. Furthermore, shear introduces strong anisotropy in the Green's function as may be anticipated from the sketch of shear-induced distortion of sound waves, Fig. 1. The Green's function shows a secular damping trend in addition to oscillations, Fig. 11. Upstream propagating waves may exhibit transient amplification as shown in Fig. 11(b); however, the response of waves in all directions eventually do not show amplification after $St > 2-4$. Waves propagating in the cross-stream x_2 direction do not suffer any change in amplitude or frequency. An increase in M_t decreases the amplitude and time scale of the oscillations while increasing the wave number also has the same effect.

The exact Green's function along with assumptions of an exponential form for temporal decorrelation, the Kolmogorov $k^{-5/3}$ law for the isotropic energy spectrum, and the $k^{-7/3}$ law for the anisotropic energy spectrum, were employed by Thacker *et al.*(2007) to calculate the rapid pressure-strain correlation. The (M_g, M_t) values were chosen to be representative of a mixing layer in one set of calculations and of a boundary layer in another set. It was found that, when $0 < M_t < 0.4$, the boundary layer values led to a large reduction of the pressure-strain correlation while the mixing layer values did not. The reason is that the boundary layer length scale near the wall is small leading to smaller M_g and weaker influence of the acoustic mode, specifically, the influence of the wave operator in the pressure equation.

SUPERSONIC CHANNEL FLOW

The influence of compressibility on wall-bounded turbulent flows, at least up to $M = 5$, is found to be mainly due to variation in mean properties. A comprehensive review of laboratory data on subsonic and supersonic boundary layers and inferred conclusions about compressibility effects is given in the monograph of Smits and Dussauge (2006). Here, results from DNS of supersonic channel flow with cooled walls are summarized.

The first DNS of supersonic channel flow was performed at $(M, Re) = (1.5, 3000), (3, 4880)$ by Coleman, Kim and Moser (1995). In this model problem, the flow is driven by a spatially constant, streamwise body force $\mathbf{f} = f\delta_{i1}$ on the r.h.s. of the momentum equation, Eq. (2), instead of a mean pressure gradient i.e. $d\langle p \rangle / dx = 0$. The walls are kept at a constant temperature lower than the adiabatic temperature so that there is heat transfer from the fluid to the walls. Since the streamwise and spanwise gradient of all mean variables is zero, the turbulence is homogeneous in these directions and statistics depend only on the wall-normal x_2 (y) direction. Owing to the cooled walls and the viscous heating, the temperature increases from its wall value leading to large property changes in the near-wall region, see Fig. 12.

Coleman *et al.*(1995) assessed the applicability of Morkovin's hypothesis that, in supersonic boundary layers, turbulence statistics appropriately normalized by the mean density, would be unaffected by Mach number and also tested the underlying assumptions. The first assumption that pressure fluctuations are small relative to other thermo-

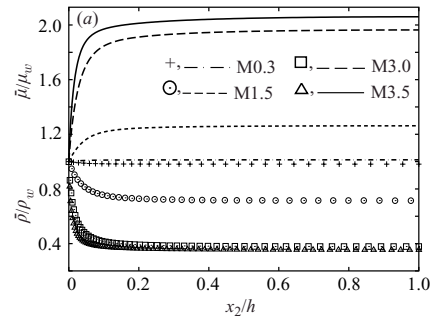


Figure 12: Wall-normal variation of mean viscosity (lines) and mean density (symbols) in supersonic channel flow with cooled walls. From Foysi *et al.*(2004).

Case	M	Re	Re $_{\tau}$	N $_{x1}$	N $_{x2}$	N $_{x3}$
M0.3	0.3	2820	181	192	129	160
M1.5	1.5	3000	221	192	151	128
M3.0	3.0	6000	556	512	221	256
M3.5	3.5	11310	1030	512	301	256

Table 3: DNS of supersonic channel flow: flow and computational parameters. From Foysi, Sarkar and Friedrich (2004).

dynamic fluctuations is borne out. The second assumption that fluctuations in total temperature, $T'_0 / \langle T_0 \rangle$, is negligible is only marginally satisfied since the r.m.s value of this quantity approaches 20% at $M = 3$. Nevertheless, normalized turbulence statistics such as

$$\frac{-\langle \rho \rangle R_{12}}{\tau_w}, \quad l = \frac{\langle u'_1 u'_2 \rangle^{1/2}}{d \langle u_1 \rangle / dx_2} \quad (23)$$

were found not to be affected by M lending support to Morkovin's hypothesis. Since l is uninfluenced by M , it immediately follows that the Van-Driest transformation,

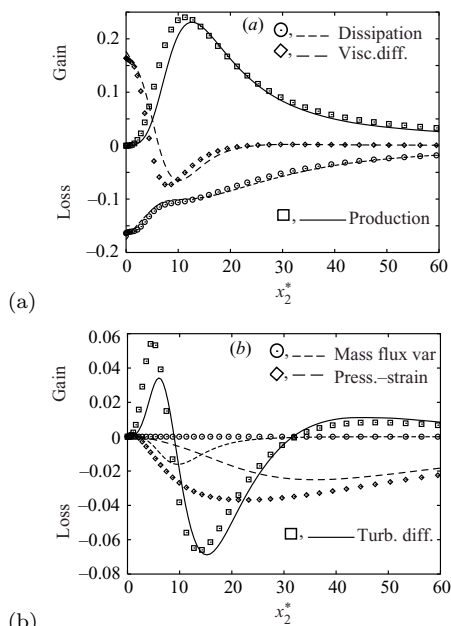
$$\langle u \rangle_{1,VD}^+ = \int_0^{\bar{u}_1^+} \sqrt{\bar{\rho} / \rho_w} d\bar{u}_1, \quad (24)$$

will lead to a log law in $\langle u \rangle_{1,VD}^+ (x_2^+)$ with incompressible boundary layer values: $\kappa \simeq 0.41, B \simeq 5.0$. The DNS data were in reasonable agreement with such a log law. The thermodynamic fluctuations were mostly non-acoustic although there was a superposed low-mode acoustic signature. It was also found that a semi-local inner scaling, based on wall shear stress and local mean properties,

$$x_2^* = \frac{x_2 u_{\tau}^*}{\langle \mu \rangle / \langle \rho \rangle} = \frac{x_2 \sqrt{\tau_w / \langle \rho \rangle}}{\langle \mu \rangle / \langle \rho \rangle}, \quad (25)$$

led to better collapse of turbulence profiles than the use of $x_2^+ = x_2 u_{\tau} / \nu$. In a companion paper (Huang, Coleman, and Bradshaw 1995), the DNS database was further interrogated. These authors found that the contribution of $\langle p'd' \rangle$ and ϵ_d to the K -balance was small, order 1 %, compared to the 10-15% contribution in uniform shear flow. Furthermore, they found that the strong Reynolds analogy, $T' \propto -u'$, was violated because of significant variation in the total temperature and proposed a modification.

Foysi, Sarkar and Friedrich (2004) examined the inner and outer scalings of the turbulent stresses, $\langle \rho \rangle R_{ij}$, in supersonic channel flow, parameters as shown in Table 3. To discriminate between M and Re effects, these authors used incompressible cases I1, I2 and I3 at $Re_{\tau} = 180, 395, 590$, respectively, from Moser, Kim and Mansour (1999). They found that the use of x_2^* instead of x_2^+ collapsed the location of the peak stresses but not the magnitude of the



(b) Figure 13: Balance of $\langle \rho \rangle R_{11}$, normalized by $\tau_w^2 / \langle \mu \rangle$, with symbols representing incompressible case I3 and lines case M3.0: (a) Production, dissipation, and viscous diffusion, and (b) Pressure strain, turbulent diffusion, and mass flux variation. Cases I3 and M3 have similar Re_τ . From Foysi *et al.*(2004).

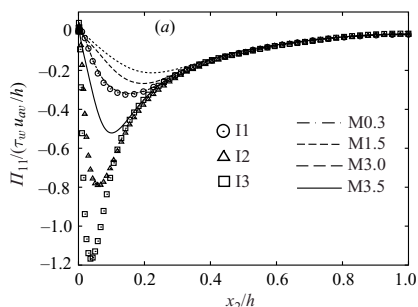


Figure 14: The pressure-strain correlation, 11-component, plotted using outer scaling. From Foysi *et al.*(2004).

peaks. The turbulence transport equations were examined. The balance of $\langle \rho \rangle R_{11}$ in Fig 13(a) shows that the dominant terms in the near-wall region, namely, the production, dissipation and viscous diffusion do not change significantly between cases I3 and M3.0. However, as shown by Fig. 13(b), the pressure-strain correlation, Π_{11} is reduced with respect to the incompressible case. This is the reason why peak $\langle \rho \rangle R_{11}$ is also larger by about 15% at $M = 3$ relative to I3.

Π_{11} , over the half-channel width, is plotted in Fig. 14. In the core of the channel, all cases collapse since the gradient in mean properties is negligible in that region. However, near the wall, Π_{11} is systematically lower in the supersonic cases. This is not a low- Re effect since case M3.5 has $Re_\tau = 1030$. The reason for this compressibility effect needs explanation. The wave operator in the p' equation can be ruled out since both M_g and M_t do not exceed 0.3 and, furthermore, the acoustic mode was found to be small compared to the entropy mode in the near-wall region. A heuristic argument and a Green's function analysis has been used to show that the reduction of pressure-strain is a *mean density* effect. Solution for the pressure at a point involves inversion of the Laplacian leading to a space integral of the source; this source includes the mean density as can be seen from the

r.h.s of Eq. (22). Consider the wall pressure. It is determined by the entire turbulent “eddy” in the vicinity of the wall and includes fluid of mean density lower than that at the cooled wall. Therefore the effective density, ρ_e , must be smaller than $\langle \rho \rangle$ and so must the pressure-strain be relative to the constant-density case. This qualitative argument was made mathematically precise by utilizing a Green's function for the Poisson equation in channel flow, see Foysi *et al.*(2004) for details.

CONCLUDING REMARKS

Compressible turbulence can be conceptually viewed as vorticity interacting with an acoustic and an entropy mode. A split of the velocity component into dilatational and solenoidal velocity is also useful. The fluctuating dilatation is small in all the flows considered here. However, since the dilatation is multiplied by the reference pressure, see Eq. (14), small dilatation does not mean that it's effect on fluctuating pressure is small. Indeed, pressure satisfies a wave equation and, as shown by Eq. (22), the wave operator cannot be neglected if M_t or M_g are $O(1)$. In uniform shear flow and in the mixing layer, M_g is $O(1)$ and r.m.s pressure fluctuations, normalized using the characteristic velocity, are found to decrease. This, in turn, leads to inhibition of the turbulence intensities and shear stress.

High-speed wall-bounded flows are inevitably accompanied by large mean temperature gradients and the dominant influence on the turbulence is due to changes in mean density and viscosity. The thermodynamic fluctuations in the boundary layer are, for the most part, associated with the entropy mode. Appropriate mean density-weighted scaling can account for some observations: the Van Driest transformation that leads to a log law and semi-local (local mean density and viscosity combined with wall value of viscous stress) scaling for the turbulence statistics. However, the pressure is non-local and, owing to its dependence on a spatial integral involving the density, correlations involving pressure cannot be collapsed using a local mean density.

ACKNOWLEDGEMENT

I would like to acknowledge the contributions of my past and ongoing collaborations over the years: with G. Erlebacher, T.B. Gatski, M. Y. Hussaini and the late C. Speziale during my initial foray into compressible turbulence at ICASE/NASA LaRC and, later, with H. Foysi, R. Friedrich, C. Pantano and W. D. Thacker. I also thank H. Foysi for his comments on this manuscript. The research has been supported by NASA and AFOSR.

*

References

- Bertoglio, J. P., F. Bataille, and J. D. Marion (2001). Two-point closures for weakly compressible turbulence. *Phys. Fluids* 13, 290–310.
- Blaisdell, G. A., N. N. Mansour, and W. C. Reynolds (1991). Numerical simulation of compressible homogeneous turbulence. *Rep. TF-50*.
- Blaisdell, G. A., N. N. Mansour, and W. C. Reynolds (1993). Compressibility effects on the growth and structure of homogeneous turbulent shear flow. *J. Fluid Mech.* 256, 443–485.

- Borodai, S. G. and R. D. Moser (2001). The numerical decomposition of turbulent fluctuations in a compressible boundary layer. *Theoret. Comput. Fluid Dyn.* 15, 35–63.
- Bradshaw, P. (1977). Compressible turbulent shear layers. *Annu. Rev. Fluid Mech.* 9, 33–54.
- Cai, X. D., E. E. O’Brien, and F. Ladiende (1997). Thermodynamic behavior in decaying, compressible turbulence with initially dominant temperature fluctuations. *Phys. Fluids* 9, 1754–1763.
- Chassaing, P., R. A. Antonia, F. Anselmet, L. Joly, and S. Sarkar (2002). *Variable density fluid turbulence*. Dordrecht: Kluwer.
- Clemens, N. T. and M. G. Mungal (1995). Large-scale structure and entrainment in the supersonic mixing layer. *J. Fluid Mech.* 284, 171–216.
- Coleman, G. N., J. Kim, and R. Moser (1995). Turbulent supersonic isothermal-wall channel flow. *J. Fluid Mech.* 305, 159–183.
- Debisschop, J. R. and J. P. Bonnet (1993). Mean and fluctuating velocity measurements in supersonic mixing layers. In W. Rodi and F. Martelli (Eds.), *Engineering Turbulence Modeling and Experiments 2*. Elsevier Science Publishers.
- Elliot, G. S. and M. Samimy (1990). Compressibility effects in free shear layers. *Phys. Fluids A* 2(7), 1231–1240.
- Erlebacher, G., M. Y. Hussaini, H. O. Kreiss, and S. Sarkar (1990). The analysis and simulation of compressible turbulence. *Theoret. Comput. Fluid Dyn.* 2, 73–95.
- Feiereisen, W. J., W. C. Reynolds, and J. H. Ferziger (1981). Numerical simulation of a compressible homogeneous shear flow. *Rep. TF-13*.
- Foysi, H. and S. Sarkar (2007). The compressible shear layer: an LES study, in preparation.
- Foysi, H., S. Sarkar, and R. Friedrich (2004). Compressibility effects and turbulence scaling in supersonic channel flow. *J. Fluid Mech.* 509, 207–216.
- Freund, J. B., S. K. Lele, and P. Moin (2000). Compressibility effects in a turbulent annular mixing layer. part 1. turbulence and growth rate. *J. Fluid Mech.* 421, 229–267.
- Friedrich, R. and F. P. Bertolotti (1997). Compressibility effects due to turbulent fluctuations. *Appl. Sci. Res.* 57, 165–194.
- Hall, J. L., P. E. Dimotakis, and H. Rosemann (1993). Experiments in Nonreacting Compressible Shear Layers. *AIAA Journal* 31(12), 2247–2254.
- Hamba, F. (1999). Effects of pressure fluctuations on turbulence growth in compressible homogeneous shear flow. *Phys. Fluids* 11, 1623–1635.
- Huang, P., G. N. Coleman, and P. Bradshaw (1995). Compressible turbulent channel flow: Dns results and modelling. *J. Fluid Mech.* 305, 185–218.
- Kovaszny, L. S. G. (1953). Turbulence in supersonic flow. *J. Aero. Sci.* 20, 657–682.
- Lee, S., S. K. Lele, and P. Moin (1991). Eddy shocklets in decaying compressible turbulence. *PF* 3, 657–664.
- Lele, S. K. (1994). Compressibility effects on turbulence. *Annu. Rev. Fluid Mech.* 26, 211–254.
- Lighthill, M. J. (1952). On sound generated aerodynamically i. general theory. *Proc. Roy. Soc. A.* 211, 564–587.
- Pantano, C. and S. Sarkar (2002). A study of compressibility effects in the high-speed turbulent shear layer using direct simulation. *J. Fluid Mech.* 451, 329–371.
- Papamoshcou, D. and A. Roshko (1988). The compressible turbulent shear layer: an experimental study. *J. Fluid Mech.* 197, 453–477.
- Passot, T. and A. Poquet (1987). Numerical simulation of compressible homogeneous flows in the turbulent regime. *J. Fluid Mech.* 181, 441–466.
- Rehm, R. G. and H. R. Baum (1978). The equations of motion for thermally-driven, buoyant flows. *J. Res. Natl. Bur. Stand.* 83, 297–308.
- Ristorcelli, J. R. (1997). A pseudo-sound constitutive relationship for the dilatational covariances in compressible turbulence. *J. Fluid Mech.* 347, 37–70.
- Ristorcelli, J. R. and G. Blaisdell (1997). Consistent initial conditions for the dns of compressible turbulence. *Phys. Fluids* 9, 4–6.
- Sarkar, S. (1992). The pressure-dilatation correlation in compressible flows. *Phys. Fluids* 4, 2674–2682.
- Sarkar, S. (1995). The stabilizing effect of compressibility in turbulent shear flow. *J. Fluid Mech.* 282, 163–186.
- Sarkar, S. (1996). On density and pressure fluctuations in uniformly sheared compressible flow. In L. Fulachier, J. L. Lumley, and F. Anselmet (Eds.), *Proc. IUTAM Symp. on Variable Density Low-Speed Flows*.
- Sarkar, S., G. Erlebacher, and M. Y. Hussaini (1991). Direct simulation of compressible turbulence in a shear flow. *Theoret. Comput. Fluid Dyn.* 2, 291–305.
- Sarkar, S., G. Erlebacher, M. Y. Hussaini, and H. O. Kreiss (1991). The analysis and modelling of dilatational terms in compressible turbulence. *J. Fluid Mech.* 227, 473–493.
- Simone, A., G. N. Coleman, and C. Cambon (1997). The effect of compressibility on turbulent shear flow: a rapid-distortion-theory and direct-numerical-simulation study. *J. Fluid Mech.* 330, 307–338.
- Smits, A. J. and J. P. Dussauge (2006). *Turbulent Shear Layers in Supersonic Flow*. New York: 2nd edition, American Institute of Physics.
- Thacker, W. D., S. Sarkar, and T. B. Gatski (2007). Analyzing the effect of compressibility on the rapid pressure-strain correlation in turbulent shear flows. *Theoret. Comput. Fluid Dyn.* 21, 171–199.
- Vreman, A. W., N. D. Sandham, and K. L. Luo (1996). Compressible mixing layer growth rate and turbulence characteristics. *J. Fluid Mech.* 320, 235–258.
- Zeman, O. (1990). Dilatational dissipation: The concept and application in modeling compressible mixing layers. *Phys. Fluids A* 2, 178–188.
- Zeman, O. (1991). On the decay of compressible turbulence. *Phys. Fluids* 3, 951–955.